

# A Deep Ordinal Distortion Estimation Approach for Distortion Rectification

Kang Liao, Chunyu Lin, Yao Zhao, *Senior Member, IEEE*

**Abstract**—Distortion is widely existed in the images captured by popular wide-angle cameras and fisheye cameras. Despite the long history of distortion rectification, accurately estimating the distortion parameters from a single distorted image is still challenging. The main reason is these parameters are implicit to image features, influencing the networks to fully learn the distortion information. In this work, we propose a novel distortion rectification approach that can obtain more accurate parameters with higher efficiency. Our key insight is that distortion rectification can be cast as a problem of learning an *ordinal distortion* from a single distorted image. To solve this problem, we design a local-global associated estimation network that learns the ordinal distortion to approximate the realistic distortion distribution. In contrast to the implicit distortion parameters, the proposed ordinal distortion have more explicit relationship with image features, and thus significantly boosts the distortion perception of neural networks. Considering the redundancy of distortion information, our approach only uses a part of distorted image for the ordinal distortion estimation, showing promising applications in the efficient distortion rectification. To our knowledge, we first unify the heterogeneous distortion parameters into a learning-friendly intermediate representation through ordinal distortion, bridging the gap between image feature and distortion rectification. The experimental results demonstrate that our approach outperforms the state-of-the-art methods by a significant margin, with approximately 23% improvement on the quantitative evaluation while displaying the best performance on visual appearance.

**Index Terms**—Distortion Rectification, Neural Networks, Learning Representation, Ordinal Distortion

## I. INTRODUCTION

Images captured by wide-angle camera usually suffer from a strong distortion, which influences the important scene perception tasks such as the object detection [1], [2] and semantic segmentation [3], [4]. The distortion rectification tries to recover the real geometric attributes from distorted scenes. It is a fundamental and indispensable part of image processing, which has a long research history extending back 60 years. In recent, distortion rectification through deep learning has attracted increasing attention [5]–[11].

Accurately estimating the distortion parameters derived from a specific camera, is a crucial step in the field of distortion rectification. However, there are two main limitations that make the distortion parameters learning challenging. (i) The distortion parameters are not observable and hard to learn from a single distorted image, such as the principal

point and distortion coefficients. Compared with the intuitive targets, such as the object classification and bounding box detection studied in other regions, the distortion parameters have more complicated and implicit relationship with image features. As a result, the neural networks obtain an ambiguous and insufficient distortion perception, which leads to inaccurate estimation and poor rectification performance. (ii) The different components of distortion parameters have different magnitudes and ranges of values, showing various effects on the global distortion distribution of an image. Such a heterogeneous representation confuses the distortion cognition of neural networks and causes a heavy imbalance problem during the training process.

To overcome the above limitations of distortion parameters estimation, previous methods exploit more guided features such as the semantic information and distorted lines [6], [7], or introduce the pixel-wise reconstruction loss [8]–[10]. However, the extra features and supervisions impose increased memory/computation cost. In this work, we would like to draw attention from the traditional calibration objective to a learning-friendly perceptual target. The target is to unify the implicit and heterogeneous parameters into an intermediate representation, thus bridging the gap between image feature and distortion estimation in the field of distortion rectification.

In particular, we redesign the whole pipeline of deep distortion rectification and present an intermediate representation based on the distortion parameters. The comparison of the previous methods and the proposed approach is illustrated in Fig. 1. Our key insight is that distortion rectification can be cast as a problem of learning an *ordinal distortion* from a distorted image. The ordinal distortion indicates the distortion levels of a series of pixels, which extend outward from the principal point. To predict the ordinal distortion, we design a local-global associated estimation network that is optimized with an ordinal distortion loss function, in which a distortion-aware perception layer is exploited to boost the features extraction of different degrees of distortion.

The proposed learning representation offers three unique advantages. First, the ordinal distortion is directly perceivable from a distorted image, it solves a simpler estimation problem than the implicit metric regression. As we can observe, the farther the pixel is away from the principal point, the larger the distortion degree is, and vice versa. This prior knowledge enables the neural networks to build a clear cognition with respect to the distortion distribution. Thus, the learning model gains more sufficient distortion perception of image features and shows faster convergence, without any extra features and pixel-wise supervisions.

Kang Liao, Chunyu Lin, Yao Zhao are with the Institute of Information Science, Beijing Jiaotong University, Beijing 100044, China, and also with the Beijing Key Laboratory of Advanced Information Science and Network Technology, Beijing 100044, China (email: kang\_liao@bjtu.edu.cn, cylin@bjtu.edu.cn, yzhao@bjtu.edu.cn).

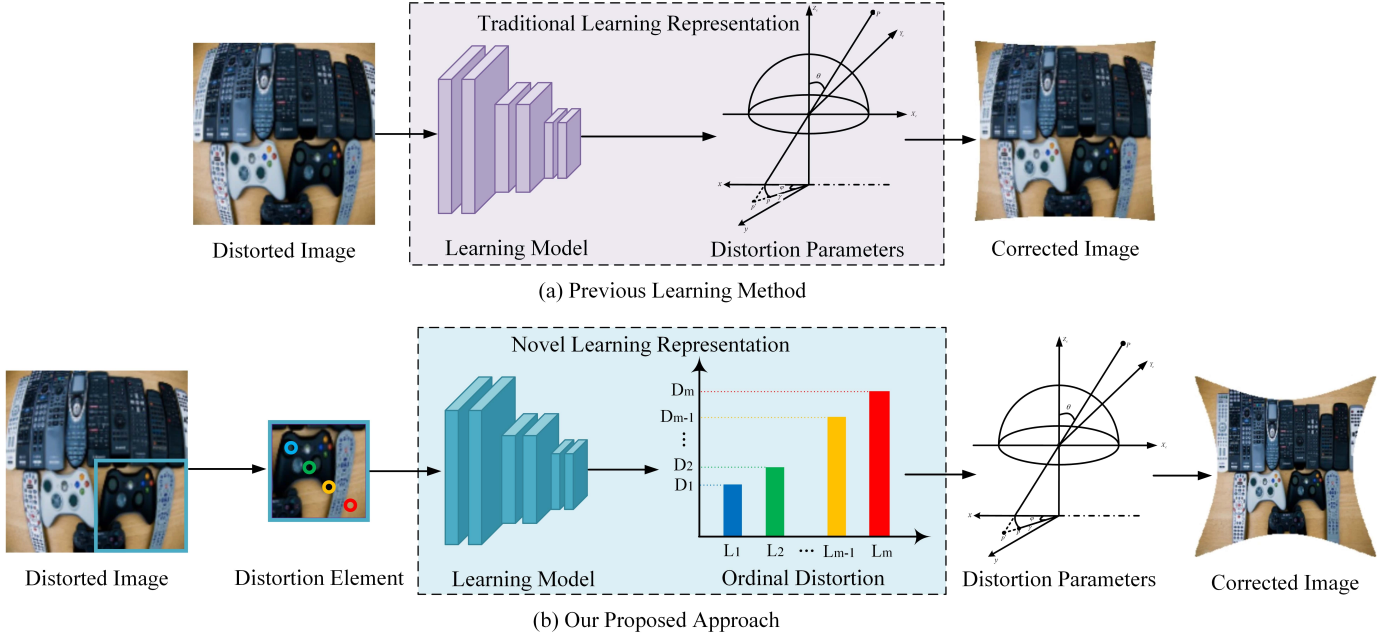


Fig. 1. Method Comparisons. (a) Previous learning methods, (b) Our proposed approach. Our aim is to transfer the traditional calibration objective into a learning-friendly representation. Previous methods roughly feed the whole distorted image into their learning models and directly estimate the implicit and heterogeneous distortion parameters. In contrast, our proposed approach only requires a part of a distorted image (distortion element) and estimates the ordinal distortion. Due to its explicit description and homogeneity, we can obtain more accurate distortion estimation and thus achieve better corrected results.

Second, the ordinal distortion is homogeneous as its all elements share a similar magnitude and description. Therefore, the imbalanced optimization problem no longer exists during the training process, and we do not need to focus on the cumbersome factor-balancing task any more. Compared to the distortion parameters with different types of components, our learning model only needs to consider one optimization objective, thus achieving more accurate estimation and more realistic rectification results.

Third, the ordinal distortion can be estimated using only a part of a distorted image. Different from the semantic information, the distortion information is redundant in images, which shows the central symmetry and mirror symmetry to the principal point. Consequently, the efficiency of rectification algorithms can be significantly improved when taking the ordinal distortion estimation as a learning target. More importantly, the ordinal relationships are invariant to monotonic transformations of distorted images, thereby increasing the robustness of the rectification algorithm.

With lots of experimental results, we verify that the proposed ordinal distortion is more suitable than the distortion parameters as a learning representation for deep distortion rectification. The experimental results also show that our approach outperforms the state-of-the-art methods with a large margin, approximately 23% improvement on the quantitative evaluation while using fewer input images, demonstrating its efficiency on distortion rectification.

The rest of this paper is organized as follows. We first introduce the related work in Section II. We then present our approach in Section III. The experiments are provided in Section IV. Finally, we conclude this paper in Section V.

## II. RELATED WORK

In this section, we briefly review the previous distortion rectification methods and classify these methods into two groups, which are the traditional vision-based one and the deep learning one.

### A. Traditional Distortion Rectification

There is a rich history of exploration in the field of distortion rectification. The most common method is based on a specific physical model. [12]–[14] utilized a camera to capture several views of a 2D calibration pattern that covered points, corners, or other features, and then computed the distortion parameters of the camera. However, these methods cannot handle images captured by other cameras and thus are restricted to the application scenario. Self-calibration was leveraged for distortion parameter estimation in [15]–[17]; however, the authors failed in the geometry recovery using only a single image. To overcome the above limitations and achieve automatic distortion rectification, Bukhari et al. [18] employed a one-parameter camera model [19] and estimated distortion parameters using the detected circular arcs. Similarly, [20], [21] also utilized the simplified camera model to correct the radial distortion in images. However, these methods perform poorly on scenes that are lacking of enough hand-crafted features. Thus, the above traditional methods are difficult to handle on the single distorted image rectification in various scenes.

### B. Deep Distortion Rectification

In contrast to the long history of traditional distortion rectification, learning methods began to study the distortion rectification in the last few years. Rong et al. [5] quantized

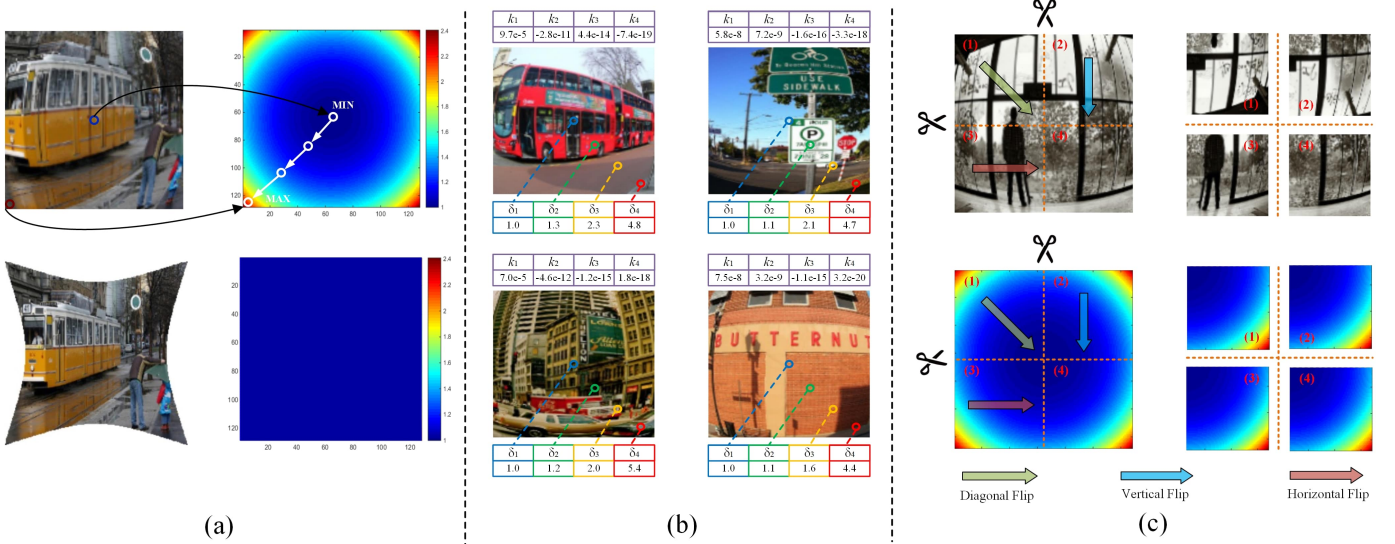


Fig. 2. Attributes of the proposed ordinal distortion. (a) Explicitness. The ordinal distortion is observable in an image and explicit to image features, which describes a series of distortion levels from small to large (top); the ordinal distortion always equals one in an undistorted image (bottom). (b) Homogeneity. Compared with the heterogeneous distortion parameters  $\mathcal{K} = [k_1 \ k_2 \ k_3 \ k_4]$ , the ordinal distortion  $\mathcal{D} = [\delta_1 \ \delta_2 \ \delta_3 \ \delta_4]$  is homogeneous, representing the same concept of distortion distribution. (c) Redundancy. After different flip operations, although the semantic features of four patches have not any relevance (top), the ordinal distortion of four patches keeps the same in distribution with each other (bottom).

the values of the distortion parameter to 401 categories based on the one-parameter camera model [19] and then trained a network to classify the distorted image. This method achieved the deep distortion rectification for the first time, while the coarse values of parameters and the simplified camera model severely influenced its generalization ability. To expand the application, Yin et al. [6] rectified the distortion in terms of the fisheye camera model using a multi-context collaborative deep network. However, their correction results heavily rely on the semantic segmentation results, leading to a strong cascading effect. Xue et al. [7] improved the performance of distortion parameter estimation by distorted lines. In analogy to traditional methods [18], [20], [21], the extra introduced hand-crafted features limit the robustness of this algorithm and decrease the efficiency of the rectification. Note that the above methods directly estimates distortion parameters from a single distorted image, such an implicit and heterogeneous calibration objective hinders the sufficient learning with respect to the distortion information. To solve the imbalance problem in the estimation of distortion parameters, recent works [8]–[10] optimized the image reconstruction loss rather than the parameters regression loss for rectification. However, their models are based on the parameter-free mechanism and cannot estimate the distortion parameters, which are important for the structure from motion and camera calibration. Manuel et al. [11] proposed a parameterization scheme for the extrinsic and intrinsic camera parameters, but they only considered one distortion coefficient for the rectification and cannot apply the algorithm into more complicated camera models.

Different from previous methods, due to the proposed learning-friendly representation, i.e., ordinal distortion, our approach can not only boost the efficient learning of neural networks and eliminate the imbalance problem, but also obtain

the accurate parameters with better rectification performance.

### III. APPROACH

In this section, we describe how to learn the ordinal distortion given a single distorted image. We first define the proposed objective in Section III-A. Next, we introduce the network architecture and training loss in Section III-B. Finally, Section III-C describes the transformation between the ordinal distortion and distortion parameter.

#### A. Problem Definition

1) *Parameterized Camera Model*: We assume that a point in the distorted image is expressed as  $\mathbf{P} = [x, y]^T \in \mathbb{R}^2$  and a corresponding point in the corrected image is expressed as  $\mathbf{P}' = [x', y']^T \in \mathbb{R}^2$ . The polynomial camera model can be described as

$$\begin{aligned} x' &= x(1 + k_1 r^2 + k_2 r^4 + k_3 r^6 + k_4 r^8 + \dots) \\ y' &= y(1 + k_1 r^2 + k_2 r^4 + k_3 r^6 + k_4 r^8 + \dots), \end{aligned} \quad (1)$$

where  $[k_1 \ k_2 \ k_3 \ k_4 \ \dots]$  are the distortion coefficients,  $r$  is the Euclidean distance between the point  $\mathbf{P}$  and the principal point  $\mathbf{C} = [x_c, y_c]^T$  in the distorted image, which can be expressed as

$$r = \sqrt{(x - x_c)^2 + (y - y_c)^2}. \quad (2)$$

This polynomial camera model fits well for small distortions but requires more distortion parameters for severe distortions. As an alternative camera model, the division model is formed by:

$$\begin{aligned} x' &= \frac{x}{1 + k_1 r^2 + k_2 r^4 + k_3 r^6 + k_4 r^8 + \dots} \\ y' &= \frac{y}{1 + k_1 r^2 + k_2 r^4 + k_3 r^6 + k_4 r^8 + \dots}. \end{aligned} \quad (3)$$



Compared with the polynomial camera model, the division model requires fewer parameters in terms of the strong distortion and thus is more suitable for the approximation of wide-angle cameras.

2) *Ordinal Distortion*: As mentioned above, most previous learning methods correct the distorted image based on the distortion parameters estimation. However, due to the implicit and heterogeneous representation, the neural network suffers from the insufficient learning problem and imbalance regression problem. These problems seriously limit the learning ability of neural networks and cause inferior distortion rectification results. To address the above problems, we propose a fully novel concept, i.e., ordinal distortion as follows. Fig. 2 illustrates the attributes of the proposed ordinal distortion.

The ordinal distortion represents the image feature in terms of the distortion distribution, which is jointly determined by the global distortion parameters and local location information. We assume that the camera model is the division model, and the ordinal distortion  $\mathcal{D}$  can be defined as

$$\mathcal{D} = [\delta(r_1) \ \delta(r_2) \ \delta(r_3) \ \cdots \ \delta(r_n)], \quad (4)$$

$$0 \leq r_1 < r_2 < r_3 < \cdots < r_n \leq R,$$

where  $R$  is the maximum distance between a point and the principal point,  $\delta(\cdot)$  indicates the distortion level of a point  $P_i$  in the distorted image:

$$\delta(r_i) = \frac{x_i}{x'_i} = \frac{y_i}{y'_i} = 1 + k_1 r_i^2 + k_2 r_i^4 + k_3 r_i^6 + k_4 r_i^8 + \cdots \quad (5)$$

Intuitively, the distortion level expresses the ratio between the coordinates of  $\mathbf{P}$  and  $\mathbf{P}'$ . The larger the distortion level is, the stronger the distortion of a pixel is, and vice versa. For an undistorted or ideally rectified image,  $\delta(\cdot)$  always equals 1. Therefore, the ordinal distortion represents the distortion levels of pixels in a distorted image, which increases outward from the principal point sequentially.

We assume the width and height of a distorted image are  $W$  and  $H$ , respectively. Then, the distortion level satisfies the following equation:

$$\begin{aligned} \delta(x_i, y_i) &= \delta(W - x_i + x_c, y_i) = \delta(x_i, H - y_i + y_c) \\ &= \delta(W - x_i + x_c, H - y_i + y_c). \end{aligned} \quad (6)$$

Thus, the ordinal distortion displays the mirror symmetry and central symmetry to the principal point in a distorted image. This prior knowledge ensures less data required in the distortion parameter estimation process.

## B. Network

1) *Network Input*: Considering the principal point is slightly disturbed in the image center, we first cut the distorted image into four patches along the center of the image, and obtain the distortion elements  $\Pi = [\pi_1 \ \pi_2 \ \pi_3 \ \pi_4]$  with size of  $\frac{H}{2} \times \frac{W}{2} \times 3$ . Although most distortion information covers in one patch, the distortion distribution of each patch is different. To normalize this diversity, we flip three of the four elements to keep the similar distortion distribution with that of the selected one. As shown in Fig. 3 and Fig. 2 (c), the top left, top right,

and bottom left distortion parts are handled with the diagonal, vertical, and horizontal flip operations, respectively.

To calculate the ordinal distortion, we further crop each distortion element into the distortion blocks  $\Theta = [\theta_1 \ \theta_2 \ \theta_3 \ \cdots \ \theta_n]$  with size of  $\frac{H}{8} \times \frac{W}{8} \times 3$  around the centers  $\Omega = [\omega_1 \ \omega_2 \ \omega_3 \ \cdots \ \omega_n]$ . To enable neural networks to explicitly learn the local distortion features, we construct the region-aware masks consisting of the bounding boxes and Gaussian blobs of the distortion blocks. Therefore, the network input includes two components. The first is the global distortion context, which provides the distortion elements with the overall distortion information and the region of interest (ROI) in which the  $\Theta$  reside. The second is the local distortion context, which provides the distortion blocks and ROI in which the  $\Omega$  reside.

2) *Network Architecture*: To jointly deduce different scales of distortion data, we design a local-global associate estimation network. As shown in Fig. 3, the network consists of two parts, a global perception module  $M_{gp}$  and a local Siamese module  $M_{ls}$ , which take the global distortion context and local distortion context as inputs, respectively.

For the global perception module, its architecture can be divided into two sub-networks, a backbone network and a header network. Specifically, the general representation of the global distortion context is extracted using the backbone network composed of convolutional layers, which indicates the high-level information including the semantic features. Any prevalent networks such as VGG16 [22], ResNet [23], and InceptionV3 [24] (without fully connected layers) can be plugged into the backbone network. We pretrain the backbone network on ImageNet [25] and fine-tune on our synthesized distorted image dataset. The header network is employed to aggregate the general representation of the input and further abstract the high-level information in the form of a feature vector, which contains three fully connected layers. The numbers of units for these layers are 4096, 2048, and 1024. The activation functions for all of the fully connected layers are ReLUs. The extracted features of the global distortion context are used to combine with the features of local distortion context, which are derived from the local Siamese module.

The local Siamese module consists of  $n$  components, each component also can be divided into a backbone network and a header network. In detail, we first use two convolutional layers to extract the low-level features with size of  $\frac{H}{32} \times \frac{W}{32} \times 256$  from the input local distortion context. Then, we feed the feature maps into a pyramid residual module consisting of five residual blocks and get the high-level features with a size of  $\frac{H}{32} \times \frac{W}{32} \times 512$ . The pyramid residual module shares the weights in each component. Subsequently, a header network with three fully connected layers aggregates the general representation of the high-level features. To comprehensively analyze the distortion information, we combine each local distortion feature with the global distortion feature and fuse these features using two fully connected layers. Finally, a fully connected layer with the unit number of  $n$  and linear activation function predicts the ordinal distortion  $\mathcal{D} = [\delta(r_1) \ \delta(r_2) \ \delta(r_3) \ \cdots \ \delta(r_n)]$  of a distorted image.

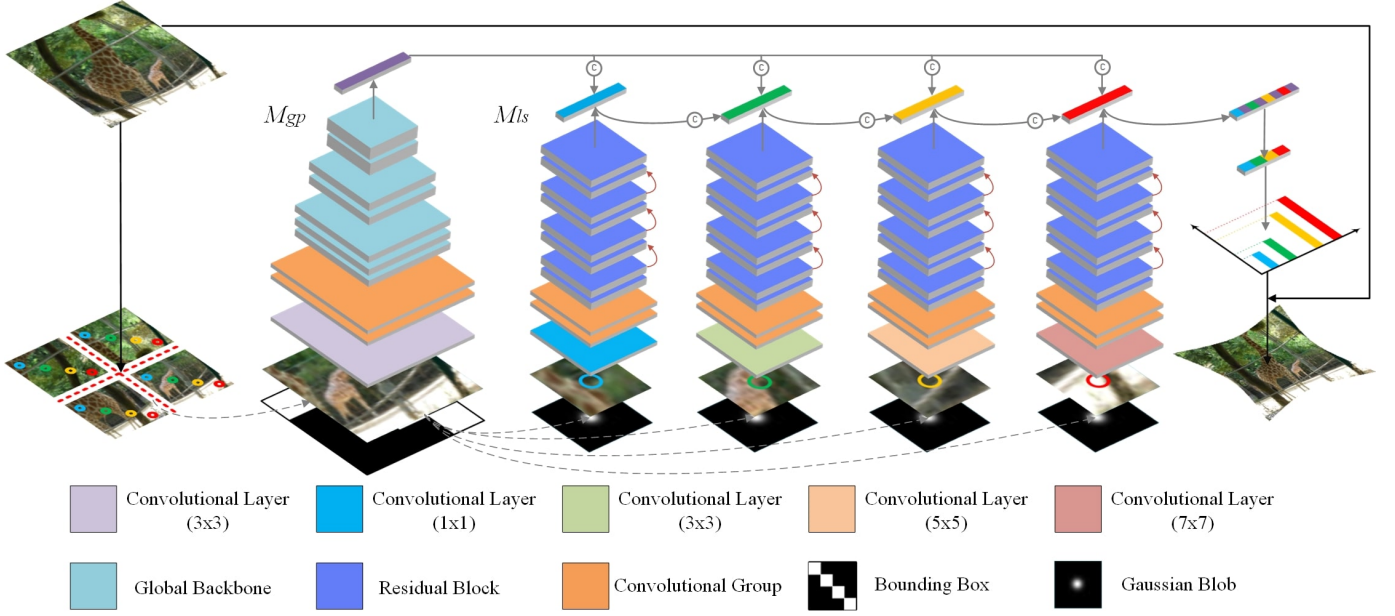


Fig. 3. Architecture of the local-global ordinal distortion estimation network. This network consists of a global perception module  $M_{gp}$  and a local Siamese module  $M_{ls}$ , jointly considering the multiple scales of distortion information given a distorted image.

In contrast to the undistorted image, the distorted image suffers from different geometric distortion in different locations. However, previous distortion rectification methods use the same size of filters to learn the overall distortion information. As a result, the learning model cannot explicitly perceive the different degrees of distortion in each distorted image and thus generates ambiguous distortion features. To enable an explicit extraction way of distortion feature, we design a distortion-aware perception layer. In general, the degree of distortion increases with the distance between the pixel and the principal point. Thus, we introduce this key prior knowledge into our learning model. Concretely, the distortion-aware perception layer is applied before feeding the input contexts to all modules. For the global distortion context, the distortion-aware perception layer leverages filters with middle size of  $W_g \times H_g$  to learn its distortion information; for the local distortion context, the distortion blocks  $\Theta = [\theta_1 \ \theta_2 \ \dots \ \theta_n]$  are processed using the filters with sizes of  $W_{l1} \times H_{l1}, W_{l2} \times H_{l2}, \dots, W_{ln} \times H_{ln}$ , from small to large. All sizes of filters satisfies the following relationship:  $W_{l1} \times H_{l1} < \dots < W_g \times H_g < \dots < W_{ln} \times H_{ln}$ . Therefore, we leverage the different sizes of filters to reason the region features with different degrees of distortions. As a benefit of the distortion-aware perception layer, our model gains improvements in regards to the distortion learning. The relevant experimental results will be described in Section IV-C.

3) *Training Loss*: After predicting the distortion labels of a distorted image, it is straightforward to use the distance metric loss such as  $\mathcal{L}_1$  loss or  $\mathcal{L}_2$  loss to learn our network parameters. However, the above loss functions cannot measure the ordered relationship between the distortion labels, while the proposed ordinal distortion possesses a strong ordinal correlation in terms of the distortion distribution. To this end, we cast the distortion estimation problem as an ordinal distortion regression problem and design an ordinal distortion

loss to train our learning model.

Suppose that the ground truth ordinal distortion  $\mathcal{D} = [\delta(r_1) \ \delta(r_2) \ \delta(r_3) \ \dots \ \delta(r_n)]$  is an increasing vector, which means  $\delta(r_1) < \delta(r_2) < \delta(r_3) < \dots < \delta(r_n)$ . Let  $\mathcal{F}_g = \varphi(I_g, \Phi)$  indicates the feature maps given a global distortion context  $I_g$ , where  $\Phi$  is the parameters involved in the backbone network of global perception module.  $\mathcal{F}_l = \{\psi_1(I_l^1, \Psi_1), \psi_2(I_l^2, \Psi_2), \dots, \psi_n(I_l^n, \Psi_n)\}$  indicate the feature maps given  $n$  local distortion context  $\{I_l^1, I_l^2, \dots, I_l^n\}$ , where  $\{\Psi_1, \Psi_2, \dots, \Psi_n\}$  are the parameters involved in the backbone networks of local Siamese module. Then,  $\chi = \eta(\mathcal{F}_g, \mathcal{F}_l, \xi)$  of size of  $n$  denotes the estimated ordinal distortion given a distorted image  $I$ , where  $\xi = \{\xi_1, \xi_2, \dots, \xi_n\}$  contains the weights of the fully connected layer of our network. The ordinal distortion loss  $\mathcal{L}(\mathcal{F}_g, \mathcal{F}_l, \xi)$  can be described by the average of each distortion level loss  $\mathcal{L}_d(i, \mathcal{F}_g, \mathcal{F}_l, \xi)$  over the entire sequence:

$$\begin{aligned} \mathcal{L}(\mathcal{F}_g, \mathcal{F}_l, \xi) &= -\frac{1}{n} \sum_{i=0}^{n-1} \mathcal{L}_d(i, \mathcal{F}_g, \mathcal{F}_l, \xi), \\ \mathcal{L}_d(i, \mathcal{F}_g, \mathcal{F}_l, \xi) &= \sum_{k=0}^{i-1} \log(\mathcal{P}_i^k) + \sum_{k=i}^{n-1} \log(1 - \mathcal{P}_i^k), \end{aligned} \quad (7)$$

where  $\mathcal{P}_i^k = P(\delta(r_i) > \delta(r_k))$  indicates the probability that  $\delta(r_i)$  is larger than  $\delta(r_k)$ .

### C. Ordinal Distortion to Distortion Parameter

Once the ordinal distortion is estimated by neural networks, the distortion coefficients  $\mathcal{K} = [k_1 \ k_2 \ \dots \ k_n]$  of a distorted

image can be easily obtained by

$$[k_1 \ k_2 \ \cdots \ k_n] = \begin{bmatrix} \delta(r_1) - 1 \\ \delta(r_2) - 1 \\ \vdots \\ \delta(r_n) - 1 \end{bmatrix}^T \begin{bmatrix} r_1^2 & r_2^2 & \cdots & r_n^2 \\ r_1^4 & r_2^4 & \cdots & r_n^4 \\ \vdots & \vdots & \ddots & \vdots \\ r_1^{2n} & r_2^{2n} & \cdots & r_n^{2n} \end{bmatrix}^{-1} \quad (8)$$

For clarity, we rewrite Eq. 8 as follows:

$$\mathcal{K} = \mathcal{D}^* \cdot \mathcal{R}^{-1}, \quad (9)$$

where  $\mathcal{D}^* = \tilde{\mathcal{D}} - [\underbrace{1 \ 1 \ \cdots \ 1}_n]$  and  $\tilde{\mathcal{D}}$  expresses the estimated ordinal distortion, and the location information with different powers is included in  $\mathcal{R}$ .

When the principal point is not fixed on the center of the image, we can also calculate all distortion parameters  $[x_c \ y_c \ k_1 \ k_2 \ \cdots \ k_n]$  using more distortion levels  $[\delta(r_1) \ \delta(r_2) \ \cdots \ \delta(r_n) \ \delta(r_{n+1}) \ \delta(r_{n+2})]$  based on Eq. 8.

In summary, we argue that by presenting our distortion rectification framework, we can have the following advantages.

1. The proposed ordinal distortion is a learning-friendly representation for neural networks, which is explicit and homogeneous compared with the implicit and heterogeneous distortion parameters. Thus, our learning model gains sufficient distortion perception of features and shows faster convergence. Moreover, this representation enables more efficient learning with less data required.

2. The local-global associate ordinal distortion estimation network considers different scales of distortion features, jointly reasoning the local distortion context and global distortion context. In addition, the devised distortion-aware perception layers boosts the features extraction of different degrees of distortion.

3. Our ordinal distortion loss fully measures the strong ordinal correlation in the proposed representation, facilitating the accurate approximation of distortion distribution.

4. We can easily calculate the distortion parameters with the estimated ordinal distortion in terms of the camera model. In contrast to previous methods, our method is able to handle various camera models and different types of distortion due to the unified learning representation.

#### IV. EXPERIMENTS

In this section, we first state the details of the synthetic distorted image dataset and the training process of our learning model. Subsequently, we analyse the learning representation for distortion estimation. To demonstrate the effectiveness of each module in our framework, we conduct an ablation study to show the different performance. At last, the experimental results of our approach compared with the state-of-the-art methods are exhibited, in both quantitative measurement and visual qualitative appearance.

##### A. Implementation Settings

**Dataset** We construct a standard distorted image dataset in terms of the division model discussed in Section III-A. Following the implementations of previous literature [6], [10], [26], we also use a 4<sup>th</sup> order polynomial based on Eq. 3, which is able to approximate most projection models with high accuracy. All of the distortion coefficients are randomly generated from their corresponding ranges. Our dataset contains 20,000 training images, 2,000 test images, and 2,000 validation images.

**Training/Testing Setting** We train our learning model using the constructed synthetic distorted images. We set the learning rate to  $5 \times 10^{-4}$  and reduce it by a factor of 10 every 200K iterations. Adam [27] is chosen as the optimizer. In the training stage, we crop each distorted image into four distortion elements and learn the parameters of neural network using all data. In the test stage, we only need one distortion element, i.e., 1/4 of an image, to estimate the ordinal distortion.

**Evaluation Metrics** Crucially, evaluating the performance of different methods with reasonable metrics benefits experimental comparisons. In the distortion rectification problem, the corrected image can be evaluated with the peak signal-to-noise ratio (PSNR) and the structural similarity index (SSIM). For the evaluation of the estimated distortion label, it is straightforward to employ the root mean square error (RMSE) between the estimated parameters  $\tilde{\mathcal{K}}$  and ground truth parameters  $\mathcal{K}$ :

$$RMSE = \frac{1}{N} \sum_{i=1}^N \sqrt{(\tilde{\mathcal{K}}_i - \mathcal{K}_i)^2}, \quad (10)$$

where  $N$  is the number of estimated distortion parameters. However, we found that different groups of distortion parameters may display similar distortion distributions in images. To more reasonably evaluate the estimated distortion labels, we propose a new metric based on the reprojection error, mean distortion level deviation (MDLD):

$$MDLD = \frac{1}{WH} \sum_{i=1}^W \sum_{j=1}^H |\delta(\tilde{i}, j) - \delta(i, j)|, \quad (11)$$

where  $W$  and  $H$  are the width and height of a distorted image, respectively. The ground truth distortion level  $\delta(i, j)$  of each pixel can be obtained using Eq. 5.

In contrast to RMSE, MDLD is more suitable for parameter evaluation due to the uniqueness of the distortion distribution. Moreover, RMSE fails to evaluate the different numbers and attributes of estimated parameters with respect to the different camera models. Thanks to the objective description of the distortion, MDLD is capable of evaluating different distortion estimation methods using different camera models.

##### B. Analysis of Learning Representation

Previous learning methods directly regress the distortion parameters from a distorted image. However, such an implicit and heterogeneous representation confuses the distortion learning of neural networks and causes the insufficient perception of distortion. To bridge the gap between image feature and

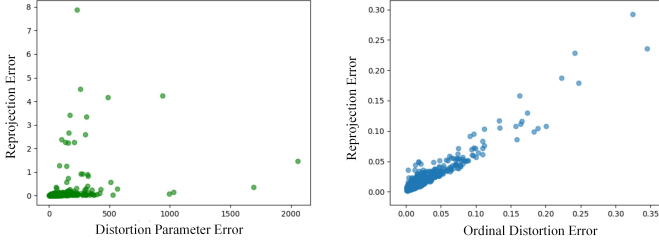


Fig. 4. Comparison of two learning representations for distortion estimation, distortion parameter (left) and ordinal distortion (right). In contrast to the ambiguous relationship between the distortion distribution and distortion parameter, the proposed ordinal distortion displays a very clear positive correlation to the distortion reprojection error.

calibration objective, we present a novel intermediate representation, i.e., ordinal distortion, which displays a learning-friendly attribute for learning models. For an intuitive and comprehensive analysis, we compare these two representations from the following three aspects.

**Relationship to Distortion Distribution** We first emphasize the relationship between two learning representations and the realistic distortion distribution of a distorted image. In detail, we train a learning model to estimate the distortion parameters and the ordinal distortions separately, and the errors of estimated results are built the relationship to the distortion reprojection error. As shown in Fig. 4, we visualize the scatter diagram of two learning representations using 1,000 test distorted images. For the distortion parameter, its relationship to the distortion distribution is ambiguous and the similar parameter errors are related to quite different reprojection errors, which indicates that optimizing the parameter error would confuse the learning of neural networks. In contrast, the ordinal distortion error displays a very clear positive correlation to the distortion distribution error, and thus the learning model gains intuitive distortion perception and the proposed representation significantly decreases the error of distortion estimation.

**Distortion Learning Evaluation** Then, we introduce three key elements for evaluating the learning representation: training data, convergence, and error. Supposed that the settings such as the network architecture and optimizer are the same, a better learning representation can be described from the less the training data is, the faster convergence and the lower error are. For example, a student is able to achieve the highest test grade (the lowest error) with the fastest learning speed and the least homework, meaning that he grasps the best learning strategy compared with other students. In terms of the above description, we evaluate the distortion parameter and ordinal distortion as shown in Fig. 5 and Fig. 6.

To comprehensively exhibit the performance, we employ three common network architectures VGG16, ResNet50, and InceptionV3 as the backbones networks of the learning model. The proposed MDLD metric is used to express the error of distortion estimation due to its unique and fair measurement for distortion distribution. To be specific, we visualize the error and convergence epoch when estimating two representations under the same number of training data in Fig. 5, which is

sampled with 20%, 40%, 60%, 80%, and 100% from the entire training data. In addition, the training and validation loss curves of two learning representations are shown in Fig. 6, in which the distortion parameters are processed without (top) and with (middle) the normalization of magnitude. From these learning evaluations, we can observe:

(1) Overall, the ordinal distortion estimation significantly outperforms the distortion parameter estimation in both convergence and accuracy, even if the amount of training data is 20% of that used to train the learning model. Note that we only use 1/4 distorted image to predict the ordinal distortion. As we pointed out earlier, the proposed ordinal distortion is explicit to the image feature and is observable from a distorted image, thus it boosts the learning ability of neural networks. On the other hand, the performance of the distortion parameter estimation drops as the amount of training data decreases. In contrast, our ordinal distortion estimation performs more consistently due to the homogeneity of the learning representation.

(2) For each backbone network, the layer depths of VGG16, InceptionV3, and ResNet50 are 23, 159, and 168, respectively. These architectures represent the different extraction abilities of image features. As illustrated in Fig. 5, the distortion parameter estimation achieves the lowest error (0.15) using InceptionV3 as the backbone under 80% training data, which indicates its performance requires more complicated and high-level features extracted by deep networks. With the explicit relationship to image features, the ordinal distortion estimation achieves the lowest error (0.07) using the VGG16 as the backbone under 100% training data. This promising performance indicates the ordinal distortion is a learning-friendly representation, which is easy to learn even using the very shallow network.

(3) From the loss curves in Fig. 6, the ordinal distortion estimation achieves the fastest convergence and best performance on the validation dataset. It is also worth to note that the ordinal distortion estimation already performs well on the validation at the first five epochs, which verifies that this learning representation yields a favorable generalization for neural networks. In contrast, suffering from the heterogeneous representation, the learning process of distortion parameter estimation displays a slower convergence. Moreover, the training and validation loss curves show unstable descend processes when the distortion parameters are handled without the normalization of magnitude, which demonstrates the distortion parameter estimation is very sensitive to the label balancing.

We further present a *learning-friendly rate* ( $\Gamma_{lr}$ ) to evaluate the effectiveness of learning representation or strategy quantitatively. To our knowledge, this is the first evaluation metric to describe the effectiveness of learning representation for neural networks. As mentioned above, the required training data, convergence, and error can jointly describe a learning representation, and thus we formulate the learning-friendly rate as follows

$$\Gamma_{lr} = \frac{1}{N} \sum_{i=1}^N \frac{D_i}{D} \left( \frac{1}{E_i} \log(2 - \frac{C_i}{C}) \right), \quad (12)$$

where  $N$  is the number of split groups,  $E_i$ ,  $D_i$ , and  $C_i$  indicate



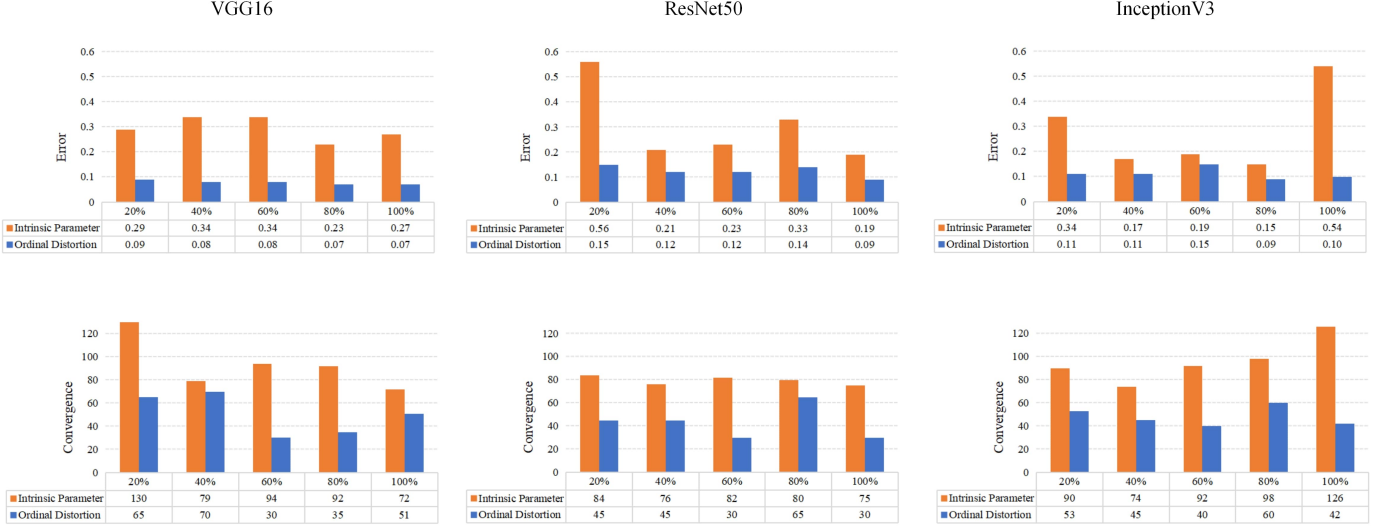


Fig. 5. Analysis of two learning representations in terms of the error and convergence. We show the histogram of error (top) and convergence (bottom) of two learning representations using three backbone networks, VGG16, ResNet50, and InceptionV3. Compared with the distortion estimation task, our proposed ordinal distortion estimation task achieves lower errors and faster convergence on all backbone networks.

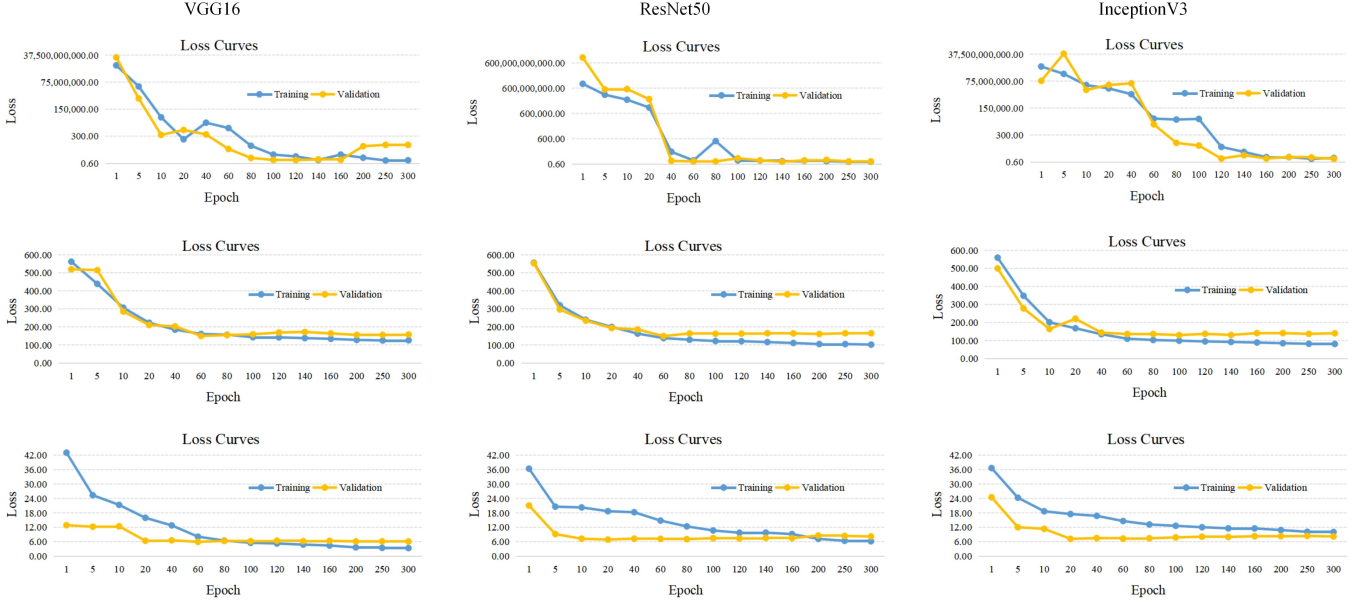


Fig. 6. Analysis of two learning representation in terms of the training and validation loss curves. We show the learning performance of the distortion parameter estimation without (top) and with (middle) the normalization of magnitude, and the ordinal distortion estimation (bottom). Our proposed ordinal distortion estimation task displays the fast convergence and stable trend on both training and validation sets.

the error, number of training data, the epoch of convergence of the  $i$ -th group, respectively.  $D$  and  $C$  indicate the total number of training data and total training epochs for the learning model. We compute the learning-friendly rates of two learning representations and list the quantitative results in Table I. The results show that our scheme outperforms the distortion parameter estimation on all backbone settings, and thus the proposed ordinal distortion is much suitable for the neural networks as a learning representation.

TABLE I  
THE LEARNING-FRIENDLY RATES OF TWO LEARNING REPRESENTATION EVALUATED WITH THREE BACKBONE NETWORKS.

Learning Representation	VGG16	ResNet50	InceptionV3
Distortion Parameter	0.50	0.60	0.59
Ordinal Distortion	<b>2.23</b>	1.43	1.50

**Qualitative Comparison** To qualitatively show the performance of different learning representations, we visualize the



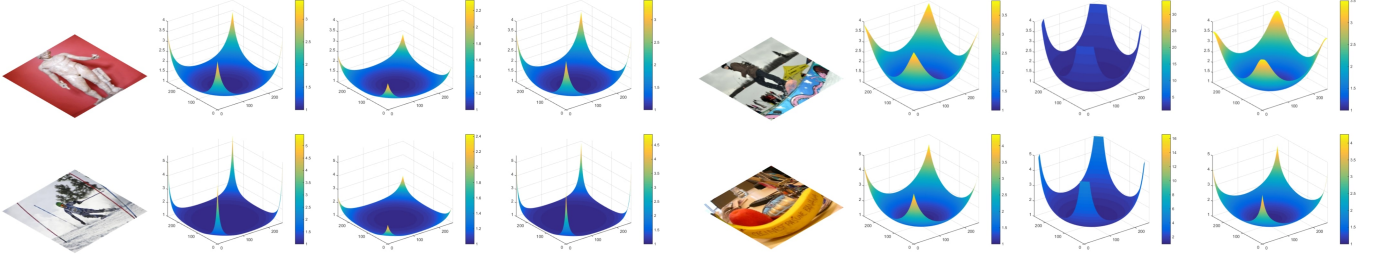


Fig. 7. Qualitative comparison of two learning representations. For each comparison, we show the distorted image, the ground truth 3D DDM, the 3D DDM constructed by the estimated distortion parameter, and ordinal distortion, from left to right.

3D distortion distribution maps (3D DDM) derived from the ground truth and these two schemes in Fig. 7, in which each pixel value of the distortion distribution map indicates the distortion level. Since the ordinal distortion estimation paid more attention to the realistic distortion perception and reasonable learning strategy, our scheme achieves results much closer to the ground truth 3D DDM. Due to implicit learning, the distortion parameter estimation generates inferior reconstructed results, such as the under-fitting (left) and over-fitting (right) on the global distribution approximation as shown in Fig. 7.

### C. Ablation Study

To validate the effectiveness of each component in our approach, we conduct an ablation study to evaluate the error of distortion estimation as shown in Fig. 8. Concretely, we first use VGG16 network without the fully connected layers as the backbone of the ordinal distortion estimation network, which is based on the analysis of the learning representation in Section IV-B. Subsequently, we implement the learning model without the flip operation (FO) on global distortion context, ordinal supervision (OS), region-aware mask (RM), and distortion-aware perception layer (DL) as the baseline (BS), and then gradually add these removed components to show the different estimation performance. In addition, we perform two loss functions:  $\mathcal{L}_2$  and  $\mathcal{L}_{sm}$  to optimize the baseline model, in which  $\mathcal{L}_{sm}$  is the smooth  $\mathcal{L}_1$  loss function [28] that combines the attributes of  $\mathcal{L}_1$  and  $\mathcal{L}_2$ . We name these two types of baseline models as BS-1 and BS-2.

Overall, the completed framework achieves the lowest error of distortion estimation as shown in Fig. 8, verifying the effectiveness of our proposed approach. For the optimization strategy, the BS-2 used  $\mathcal{L}_{sm}$  performs much better than BS-1 used  $\mathcal{L}_2$  since the  $\mathcal{L}_{sm}$  loss function boosts a more stable training process. Due to the effective normalization of distortion distribution, the network gains explicit spatial guidance with the flip operation on the global distortion context. We also show the training loss of the first 30 epochs derived from the BS-2 and BS-2 + FO in Fig. 9, where we can observe that the distribution normalization can significantly accelerate the convergence of the training process. By contrary, the BS-2 without flip operation suffers from a *confused learning period* especially in the first 10 epochs, which indicates that the neural network is unsure how to find a direct optimization way from

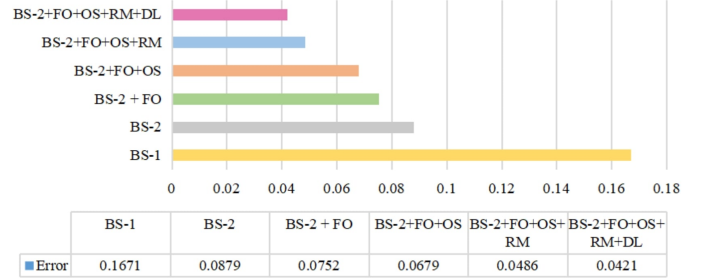


Fig. 8. Ablation study of the proposed ordinal distortion estimation approach.

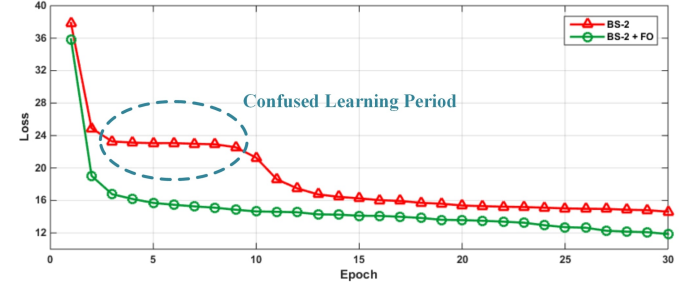


Fig. 9. Training loss of first 30 epochs derived from the BS-2 and BS-2 + FO. The flip operation that normalizes the distortion distribution of inputs is able to significantly accelerate the convergence of the learning process.

the distribution difference. Moreover, the ordinal supervision fully measures the strong ordinal correlation in the proposed representation, and thus facilitates the accurate approximation of distortion distribution. With the special attention mechanism and distortion feature extraction, our learning model gains further improvements using the region-aware mask and distortion-aware perception layer.

### D. Comparison Results

In this part, we compare our approach with the state-of-the-art methods in both quantitative and qualitative evaluations, in which the compared methods can be classified into traditional methods [20] [21] and learning methods [5] [8] [9]. Note that our approach only requires 1/4 part of a whole distorted image to estimate the distortion label, which is further employed for the subsequent image rectification.

**Quantitative Evaluation** To demonstrate a quantitative comparison with the state-of-the-art approaches, we evaluate the



Fig. 10. Qualitative evaluations of the rectified distorted images on indoor (left) and outdoor (right) scenes. For each evaluation, we show the distorted image, ground truth, and corrected results of the compared methods: Alemán-Flores [20], Santana-Cedr s [21], Rong [5], Li [8], and Liao [9], and rectified results of our proposed approach, from left to right.



Fig. 11. Qualitative evaluations of the rectified distorted images on people (left) and challenging (right) scenes. For each evaluation, we show the distorted image, ground truth, and corrected results of the compared methods: Alem n-Flores [20], Santana-Cedr s [21], Rong [5], Li [8], and Liao [9], and rectified results of our proposed approach, from left to right.

TABLE II  
QUANTITATIVE EVALUATION OF THE RECTIFIED RESULTS OBTAINED BY  
DIFFERENT METHODS.

Comparison Methods	PSNR $\uparrow$	SSIM $\uparrow$	MDLD $\downarrow$
Traditional Methods			
Alem�n-Flores [20]	9.47	0.31	0.26
Santana-Cedr�s [21]	7.90	0.25	1.18
Learning Methods			
Rong [5]	10.37	0.29	0.23
Li [8]	13.87	0.64	-
Liao [9]	20.28	0.72	-
Ours	<b>24.82</b>	<b>0.84</b>	<b>0.04</b>

rectified images using PSNR, SSIM, and the proposed MDLD. As listed in Table II, our approach significantly outperforms the compared approaches in all metrics, including the highest metrics on PSNR and SSIM, as well as the lowest metric on MDLD. Specifically, compared with the traditional methods [20], [21] based on the hand-crafted features, our approach overcomes the scene limitation and simple camera model assumption, showing more promising generality and flexibility. Compared with the learning distortion rectification methods [5] [8] [9], which ignores the prior knowledge of the distortion, our approach transfers the heterogeneous estimation problem into a homogeneous one, which also eliminates the implicit relationship between image features and predicted values in a

more explicit expression. As benefits of the effective ordinal supervision and guidance of distortion information during the learning process, our approach outperforms Liao [9] by a significant margin, with approximately 23% improvement on PSNR and 17% improvement on SSIM.

**Qualitative Evaluation** We visually compare the corrected results from our approach with those of the state-of-the-art methods using our synthetic test set and the real distorted images. To show the comprehensive rectification performance under different scenes, we split the test set into four types of scenes as indoor, outdoor, people, and challenging scenes. The indoor and outdoor scenes are shown in Fig. 10, and the people and challenging scenes are shown in Fig. 11. Our approach performs well on all scenes, while the traditional methods [20], [21] show inferior corrected results under the scene that lacks sufficient hand-crafted features, especially in the people and challenging scenes. On the other hand, the learning methods [5], [8], [9] lag behind in the sufficient distortion perception and cannot easily adapt to scenes with strong geometric distortion. For example, the results obtained by Rong [5] show coarse rectified structures, which are induced by the implicit learning of distortion and simple model assumption. Li [8] leveraged the estimated distortion flow to generate the rectified images. However, the accuracy of the pixel-wise reconstruction heavily rely on the performance of scene analysis, leading to some stronger distortion results



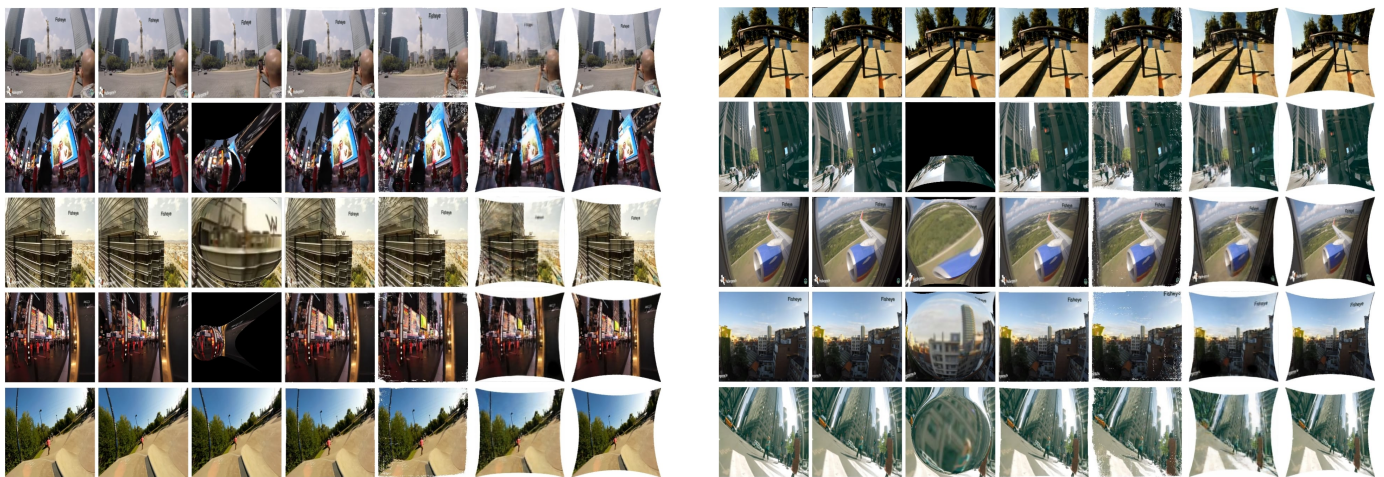


Fig. 12. Qualitative evaluations of the rectified distorted images on real scenes. For each evaluation, we show the distorted image and corrected results of the compared methods: Alemán-Flores [20], Santana-Cedrés [21], Rong [5], Li [8], and Liao [9], and rectified results of our proposed approach, from left to right.

under complex scenes. Although Liao [9] generated better rectified images than the above learning methods in terms of the global distribution, the results display unpleasing blur local appearances due to the used adversarial learning manner. In contrast, our results achieve the best performance on both global distribution and local appearance, which are benefited by the proposed learning-friendly representation and the effective learning model.

The comparison results of the real distorted image are shown in Fig. 12. We collect the real distorted images from the videos in YouTube, which are capture by popular fisheye lenses, such as the SAMSUNG 10mm F3, Rokinon 8mm Cine Lens, Opteka 6.5mm Lens, and GoPro. As illustrated in Fig. 12, our approach generates the best rectification results compared with the state-of-the-art methods, showing the appealing generalization ability for blind distortion rectification. To be specific, the salient objects such buildings, streetlight, and roads are recovered into their original straight structures by our approach, which exhibit more realistic geometric appearance than the results of other methods. Since our approach mainly focuses on the design of learning representation for distortion estimation, the neural networks gains more powerful learning ability with respect to the distortion perception and achieves more accurate estimation results.

## V. CONCLUSION

In this paper, we present a novel learning representation for the deep distortion rectification, bridging the gap between image feature and calibration objective. Compared with the implicit and heterogeneous distortion parameters, the proposed ordinal distortion offers three unique advantages such as the explicitness, homogeneity, and redundancy, which enables more sufficient and efficient learning on the distortion. To learn this representation, we design a local-global associate estimation network that is optimized with an ordinal distortion loss function, and a distortion-aware perception layer is used to boost the features extraction of different degrees of distortion.

As the benefit of the proposed learning representation and learning model, our approach outperforms the state-of-the-art methods by a remarkable margin while only leveraging 1/4 data for distortion estimation. In future work, we plan to solve other challenging computer vision tasks with a new and learning-friendly representation.

## REFERENCES

- [1] G. Li, Y. Gan, H. Wu, N. Xiao, and L. Lin, “Cross-modal attentional context learning for rgb-d object detection,” *IEEE Transactions on Image Processing*, vol. 28, no. 4, pp. 1591–1601, 2019.
- [2] P. Zhang, W. Liu, H. Lu, and C. Shen, “Salient object detection with lossless feature reflection and weighted structural loss,” *IEEE Transactions on Image Processing*, vol. 28, no. 6, pp. 3048–3060, 2019.
- [3] B. Kang and T. Q. Nguyen, “Random forest with learned representations for semantic segmentation,” *IEEE Transactions on Image Processing*, vol. 28, no. 7, pp. 3542–3555, 2019.
- [4] C. Redondo-Cabrera, M. Baptista-Ríos, and R. J. López-Sastre, “Learning to exploit the prior network knowledge for weakly supervised semantic segmentation,” *IEEE Transactions on Image Processing*, vol. 28, no. 7, pp. 3649–3661, 2019.
- [5] J. Rong, S. Huang, Z. Shang, and X. Ying, “Radial lens distortion correction using convolutional neural networks trained with synthesized images,” in *Asian Conference on Computer Vision*, pp. 35–49, 2016.
- [6] X. Yin, X. Wang, J. Yu, M. Zhang, P. Fua, and D. Tao, “FishEyeRecNet: A multi-context collaborative deep network for fisheye image rectification,” in *European Conference on Computer Vision*, pp. 469–484, 2018.
- [7] Z. Xue, N. Xue, G.-S. Xia, and W. Shen, “Learning to calibrate straight lines for fisheye image rectification,” in *Proceedings of the IEEE Conference on Computer Vision and Pattern Recognition*, pp. 1643–1651, 2019.
- [8] X. Li, B. Zhang, P. V. Sander, and J. Liao, “Blind geometric distortion correction on images through deep learning,” in *Proceedings of the IEEE Conference on Computer Vision and Pattern Recognition*, pp. 4855–4864, 2019.
- [9] K. Liao, C. Lin, Y. Zhao, and M. Xu, “Model-free distortion rectification framework bridged by distortion distribution map,” *IEEE Transactions on Image Processing*, vol. 29, pp. 3707–3718, 2020.
- [10] K. Liao, C. Lin, Y. Zhao, and M. Gabbouj, “Dr-gan: Automatic radial distortion rectification using conditional gan in real-time,” *IEEE Transactions on Circuits and Systems for Video Technology*, vol. 30, no. 3, pp. 725–733, 2020.
- [11] M. Lopez, R. Mari, P. Gargallo, Y. Kuang, J. Gonzalez-Jimenez, and G. Haro, “Deep single image camera calibration with radial distortion,” in *Proceedings of the IEEE Conference on Computer Vision and Pattern Recognition*, pp. 11817–11825, 2019.

- [12] Z. Zhang, "A flexible new technique for camera calibration," *IEEE Transactions on Pattern Analysis and Machine Intelligence*, vol. 22, 2000.
- [13] C. Mei and P. Rives, "Single view point omnidirectional camera calibration from planar grids," *IEEE International Conference on Robotics and Automation*, pp. 3945–3950, 2007.
- [14] S. Gasparini, P. F. Sturm, and J. P. Barreto, "Plane-based calibration of central catadioptric cameras," *IEEE International Conference on Computer Vision*, pp. 1195–1202, 2009.
- [15] S. B. Kang, "Catadioptric self-calibration," in *IEEE International Conference on Computer Vision*, 2000.
- [16] S. Ramalingam, P. F. Sturm, and S. K. Lodha, "Generic self-calibration of central cameras," *Computer Vision and Image Understanding*, vol. 114, pp. 210–219, 2010.
- [17] F. Espuny, "Generic self-calibration of central cameras from two rotational flows," *International Journal of Computer Vision*, vol. 91, pp. 131–145, 2007.
- [18] F. Bukhari and M. N. Dailey, "Automatic radial distortion estimation from a single image," *Journal of Mathematical Imaging & Vision*, vol. 45, no. 1, pp. 31–45, 2013.
- [19] A. W. Fitzgibbon, "Simultaneous linear estimation of multiple view geometry and lens distortion," in *IEEE Conference on Computer Vision and Pattern Recognition*, 2001.
- [20] M. Alemánflores, L. Alvarez, L. Gomez, and D. Santanacedrés, "Automatic lens distortion correction using one-parameter division models," *Image Processing on Line*, vol. 4, 2014.
- [21] D. Santana-Cedr s, L. Gomez, M. Alem n-Flores, A. Salgado, J. Esclar n, L. Mazorra, and L. Alvarez, "An iterative optimization algorithm for lens distortion correction using two-parameter models," *Image Processing On Line*, vol. 6, pp. 326–364, 2016.
- [22] K. Simonyan and A. Zisserman, "Very deep convolutional networks for large-scale image recognition," *CoRR*, vol. abs/1409.1556, 2015.
- [23] K. He, X. Zhang, S. Ren, and J. Sun, "Deep residual learning for image recognition," *IEEE Conference on Computer Vision and Pattern Recognition*, pp. 770–778, 2016.
- [24] C. Szegedy, V. Vanhoucke, S. Ioffe, J. Shlens, and Z. Wojna, "Rethinking the inception architecture for computer vision," *Proceedings of the IEEE Conference on Computer Vision and Pattern Recognition*, pp. 2818–2826, 2016.
- [25] A. Krizhevsky, I. Sutskever, and G. E. Hinton, "Imagenet classification with deep convolutional neural networks," in *Advances in Neural Information Processing Systems*, pp. 1097–1105, 2012.
- [26] D. Scaramuzza, A. Martinelli, and R. Siegwart, "A toolbox for easily calibrating omnidirectional cameras," *IEEE/RSJ International Conference on Intelligent Robots and Systems*, pp. 5695–5701, 2006.
- [27] T.-Y. Lin, M. Maire, S. Belongie, J. Hays, P. Perona, D. Ramanan, P. Doll r, and C. L. Zitnick, "Microsoft coco: Common objects in context," in *European Conference on Computer Vision*, pp. 740–755, 2014.
- [28] S. Ren, K. He, R. Girshick, and J. Sun, "Faster R-CNN: Towards real-time object detection with region proposal networks," *IEEE Transactions on Pattern Analysis and Machine Intelligence*, no. 6, pp. 1137–1149, 2017.